# Porphyrins. 36.[1] Synthesis and Optical and Electronic Properties of Some Ruthenium and Osmium Octaethylporphyrins

**Artemis Antipas,[2a] Johann W. Buchler,[2b] Martin Gouterman,*[2a] and Paul D. Smith[2b]**

*Contribution from the Department of Chemistry, University of Washington, Seattle, Washington 98195, and the Institut für Anorganische Chemie, Technische Hochschule, D-51 Aachen, Federal Republic of Germany.*
*Received August 1, 1977*

**Abstract:** The optical absorption and emission spectra as well as their rationalization in terms of iterative extended Hückel (IEH) calculations are reported for eight $Ru^{II}$ and $Os^{II}$ complexes of octaethylporphyrin (OEP): Ru(OEP)$py_2$, Ru(OEP)-CO(py), Ru(OEP)NO(OMe) (**2a–c**); Os(OEP)$py_2$, Os(OEP)CO(py), Os(OEP)NO(OMe), Os(OEP)$[P(OMe)_3]_2$, Os(OEP)$N_2$(THF) (**3a–e**). (Here py = pyridine and THF = tetrahydrofuran.) We also report on the $Os^{IV}$ and $Os^{VI}$ complexes Os(OEP)$(OMe)_2$ (**4**) and $OsO_2$(OEP) (**5**). Improved syntheses or spectral and analytical characterizations are presented, especially for the complexes **2a–c**, **3e**, and **5**. Comparison is also made to spectra and calculations for $Fe^{II}$ porphyrin complexes with bispyridine (**1a**) and carbonylpyridine (**1b**). The absorption spectra of the $Fe^{II}$, $Ru^{II}$, and $Os^{II}$ porphyrins have blue-shifted $Q(\pi,\pi^*)$ bands, indicating metal $d_\pi \rightarrow$ porphyrin $e_g(\pi^*)$ back-bonding. All the species show evidence for extra electronic absorption bands in the visible–near UV region, which are interpreted by the IEH calculations as follows. Forbidden transitions $d \rightarrow e_g(\pi^*)$ provide hints of absorption bands for the $M^{II}$ species **2b**, **3b**, **3d**, and **3e**. Extra allowed absorption of character $a_{1u}(\pi)$, $a_{2u}(\pi) \rightarrow [NO(\pi^*) + e_g(d_\pi)]$ is apparent in **2c** and **3c**. In **4** and **5** the extra allowed absorption bands are of $a_{1u}(\pi)$, $a_{2u}(\pi) \rightarrow e_g(d_\pi)$ character. The extra allowed absorption bands for the bispyridine complexes **2a** and **3a** are attributed to doubly excited states of form $[e_g(d_\pi)]^3\,[a_{1u}(\pi),a_{2u}(\pi)]^3[e_g(\pi^*)]^2$. Four species luminesce: Ru(OEP)CO(py) (**2b**) shows phosphorescence from the ring $T_1(\pi,\pi^*)$ level with origin at 653 nm; at 77 K it shows quantum yield $\phi_p \sim 0.06$ and an exponential decay with lifetime 405 μs. Os(OEP)NO(OMe) (**3c**) shows a similar emission with origin at 688 nm; at 77 K it has $\phi_p \sim 3 \times 10^{-3}$ and a nonexponential decay that can be fit with decay times of 116 and 35 μs. At 77 K, Os(OEP)co)py) (**3b**) shows an unusual, broad, weak, short-lived emission between 720 and 780 mm with $\phi_p \sim 6 \times 10^{-4}$; this emission is attributed to a charge transfer triplet $T(d,\pi^*)$ excited state. $OsO_2$(OEP) (**5**) shows emission with origin 729 nm; at 300 K in deoxygenated solution it has $\phi_p \sim 5 \times 10^{-3}$.

## Introduction

Iron porphyrins are important as prosthetic groups for a variety of hemoproteins. They can bind many small molecules and ions, and in these complexes show a variety of absorption spectra.[3-5] Given the semiquantitative nature of electronic theory of large molecules, it would be nearly impossible to understand iron complexes alone; and only through the relationship to other metals can a sound understanding be reached. In this context comparisons of otherwise isosteric metalloporphyrins containing group homologues as central metals has revealed important details of the electronic structure.[6,7]

Table I lists the 12 Fe, Ru, and Os complexes that will be discussed in this paper and the abbreviations to be used for them. Optical absorption and emission data will be given on the ten Ru and Os complexes, and iterative extended Hückel (IEH) calculations are reported for all complexes. We shall compare the calculations on the Fe complexes to absorption spectra reported for iron mesoporphyrin IX dimethyl ester.[5] We shall also report detailed synthetic procedures and analytic characterizations for those species for which characterization has not appeared (**2c, 3a**) or for which the characterization is much improved (**2a,b, 3a, 3e, 5**).

## Experimental Section

**Materials and Methods.** (J.W.B. and P.D.S.) Elemental analyses were performed by Mikroanalytisches Laboratorium A. Bernhardt, D-5251 Elbach, West Germany. Mass spectral data were taken on a Varian CH5 (70 eV) using a direct insertion probe, temperature ca. 200 °C.

All solvents were distilled before use. Benzene and THF were dried and stored over sodium. The quantitative electronic absorption spectra were taken with spectroscopic quality solvents (Uvasol, Merck). Column chromatography was performed with $Al_2O_3$ (Woelm) or silica gel (Woelm). Preparatory thin layer chromatography was accomplished with silica gel H, type 60, Stahl (Merck), on 20 × 100 cm glass plates (0.5-mm layer thickness). Instead of melting point determination, analytical thin layer chromatography on metal cards of silica gel SI (Riedel de Haen) with $CH_2Cl_2$ or benzene was used as a criterion of purity. $Ru_3(CO)_{12}$ was purchased from Alpha Inorganics.

Carbonyl(octaethylporphinato)pyridineosmium(II) (**3b**),[8] methoxonitrosonium(octaethylporphinato)osmium(II) (**3c**),[9] octaethylporphinatobis(trimethyl phosphite)osmium(II) (**3d**),[8] bis(methoxo)(octaethylporphinato)osmium(IV) (**4**),[9] dinitrogen(octaethylporphinato)tetrahydrofuranosmium(II) (**3e**),[11] and octaethylporphinatodioxoosmium(VI) (**5**)[10] were prepared from octaethylporphyrin [$H_2$(OEP)] by the literature methods cited.

**Carbonyl(octaethylporphinato)pyridineruthenium(II) (2b).** Following earlier workers[12,13] a solution of $H_2$(OEP) (500 mg, 0.94 mmol) and 1.0 g of $Ru_3(CO)_{12}$ in 200 mL of benzene was allowed to reflux under nitrogen for 60 h. After the addition of 10 mL of pyridine, the solvent was removed by rotary evaporation and the remaining residue was chromatographed on a silica gel column (activity grade I, Woelm) by eluting with $CH_2Cl_2$. After filtration and evaporation, the desired product was crystallized from 40 mL of $CH_2Cl_2$–MeOH–pyridine (49:49:2) giving 66 mg (53%) of Ru(OEP)CO(py) (**2b**).

Anal. Calcd for $C_{42}H_{49}N_5ORu$ (740.1 g/mol): C, 68.10; H, 6.62; N, 9.46; O, 2.16. Found: C, 68.24; H, 6.53; N, 9.54; O, 2.11.

Mass spectrum: A = 634 [100%, $^{102}Ru(OEP)^+$], 317 [42%, $Ru(OEP)^{2+}$], 662 [29%, $Ru(OEP)CO^+$], 331 [11%, $Ru(OEP)CO^{2+}$].

**(Octaethylporphinato)bis(pyridine)ruthenium(II) (2a).** Modifying a procedure of Whitten et al.,[14] a solution of 100 mg (0.14 mmol) of Ru(OEP)CO(py) (**2b**) in 70 mL of pyridine was allowed to reflux under Ar for 1 h. After cooling, the solution was irradiated with a 125-W mercury lamp (Pyrex filter) for 20 h, while continually flushing the solution with Ar. The solution was then reduced to a 2-mL volume by boiling off the pyridine. After cooling, 102 mg (95%) of long, reddish-black needles of Ru(OEP)$py_2$ (**2a**) were recovered by suction filtration and washed several times with cold MeOH.

Anal. Calcd for $C_{46}H_{54}N_6Ru$ (791.1 g/mol): C, 69.78; H, 6.83; N, 10.62; O, 0.00. Found: C, 69.94; H, 6.90; N, 10.76; O, 0.00.

**Methoxonitrosonium(octaethylporphinato)ruthenium(II) (2c).** A solution of 100 mg (0.14 mmol) of Ru(OEP)CO(py) (**2b**) in 15 mL

0002-7863/78/1500-3015$01.00/0 

**Table I.** Abbreviation Scheme for the Compounds[a]

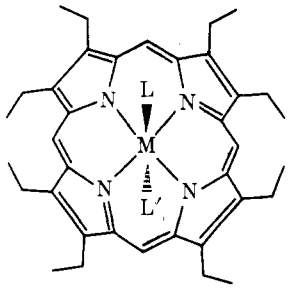

**1-5**

| No. | M | Z[b] | L | L′ | Short formula |
|---|---|---|---|---|---|
| **1a** | Fe | +2 | py | py | $Fe(OEP)py_2$ |
| **1b** | Fe | +2 | CO | py | Fe(OEP)CO(py) |
| **2a** | Ru | +2 | py | py | $Ru(OEP)py_2$ |
| **2b** | Ru | +2 | CO | py | Ru(OEP)CO(py) |
| **2c** | Ru | +2 | NO | OMe | Ru(OEP)NO(OMe) |
| **3a** | Os | +2 | py | py | $Os(OEP)py_2$ |
| **3b** | Os | +2 | CO | py | Os(OEP)CO(py) |
| **3c** | Os | +2 | NO | OMe | Os(OEP)NO(OMe) |
| **3d** | Os | +2 | $P(OMe)_3$ | $P(OMe)_3$ | $Os(OEP)[P(OMe)_3]_2$ |
| **3e** | Os | +2 | $N_2$ | THF | $Os(OEP)N_2(THF)$ |
| **4** | Os | +4 | OMe | OMe | $Os(OEP)(OMe)_2$ |
| **5** | Os | +6 | O | O | $OsO_2(OEP)_2$[c] |

[a] Abbreviations used: $(P)^{2-}$, general porphinate dianion; $(OEP)^{2-}$, octaethylporphyrinate dianion; $(Etio\text{-}I)^{2-}$, etioporphyrinate-I dianion; M, central metal; Me, $CH_3$; py, pyridine; THF, tetrahydrofuran; 3MP, 3-methylpentane; EPA, diethyl ether-isopentane-ethanol (5:2:2). [b] Z: Formal oxidation state of the central metal M. [c] Note: dioxo, not dioxygen.

of $CH_2Cl_2$ was flushed with Ar after the addition of 10 mL of MeOH, then briefly exposed to NO[9] (2 min), and then allowed to stand for 1 h. After three similar gas exposure cycles, the $Al_2O_3$ thin layer chromatogram showed complete conversion of the starting material. The solution was then flushed with Ar and evaporated to dryness. The residue was chromatographed on a column of $Al_2O_3$ (neutral, activity grade III) by eluting with $CH_2Cl_2$. Crystallization from $CH_2Cl_2$–MeOH (2:1) afforded 48 mg (55%) of Ru(OEP)NO(OMe) (**2c**).

Anal. Calcd for $C_{37}H_{47}N_5O_2Ru$ (694.1 g/mol): C, 63.97; H, 6.77; N, 10.09; O, 4.61. Found: C, 63.82; H, 6.69; N, 10.04; O, 4.69.

Mass spectrum: A = 634 [100%, $^{102}Ru(OEP)^+$], 695 [61%, $Ru(OEP)NO(OMe)^+$], 664 [36%, $Ru(OEP)NO^+$], 332 [17%, $Ru(OEP)NO^{2+}$], 317 [12%, $Ru(OEP)^{2+}$], 347.5 [7%, $Ru(OEP)NO(OMe)^{2+}$].

**(Octaethylporphinato)bis(pyridine)osmium(II) (3a).** To a boiling solution of $OsO_2(OEP)$ (**5**, 60 mg, 0.08 mmol) in 20 mL of THF contained in a 50-mL beaker under atmospheric conditions 3 drops of hydrazine hydrate (100%) was added. The color of the solution turned from olive green to orange red. At this point, 15 mL of pyridine was added and the volume of the solution was reduced to 5 mL by distilling off the solvent. After cooling, 60 mg (86%) of the desired $Os(OEP)py_2$ (**3a**) was recovered by suction filtration and washed several times with cold methanol.

Anal. Calcd for $C_{46}H_{54}N_6Os$ (880.2 g/mol): C, 62.71; H, 6.13; N, 9.54; O, 0.00. Found: C, 62.60; H, 6.54; N, 9.73; O, 0.21.

Mass spectrum: A = 724 [100%, $^{192}Os(OEP)^+$], 362 [90%, $Os(OEP)^{2+}$], 441 [19%, $Os(OEP)py_2^{2+}$], 882 [12%, $Os(OEP)py_2^+$], 401.5 [6%, $Os(OEP)py^{2+}$].

**Dinitrogen(octaethylporphinato)tetrahydrofuranosmium(II) (3e).**[11] Anal. Calcd for $C_{40}H_{52}N_6OOs(H_2O)$ (841.1 g/mol): C, 57.12; H, 6.47; N, 9.99; O, 3.80. Found: C, 58.33; H, 6.52; N, 9.95; O, 3.80.

**Octaethylporphinatodioxoosmium(VI) (5).**[10] Anal. Calcd for $C_{36}H_{44}N_4O_2Os$ (754.2 g/mol): C, 57.27; H, 5.87; N, 7.42; O, 4.24. Found: C, 58.27; H, 6.34; N, 7.23; O, 4.27.

NMR data are given in Table II.

**Measurement of Optical Emission** (A.A., M.G., and P.D.S.) Our emission apparatus has been described previously.[15] An additional new feature was that the data were fed via an a-d converter into a PDP 8/e computer, which plotted the uncorrected as well as the corrected spectra on a Calcomp-565. The emission spectra were corrected for the monochromator and photomultiplier tube wavelength sensitivity. Excitation spectra were taken for all emission peaks and all the reported emission peaks belonged to the main absorbing species. Occasional weak emission was observed from species reported as nonemitting, but all such emissions were shown by excitation spectra to belong to impurities.

Our solvent of choice for emission studies was 3-methylpentane, which is particularly inert and forms a glass at 77 K. However, because of insolubility, we used EPA (ethyl ether-isopentane-ethanol, 5:5:2) for $Os(OEP)(OMe)_2$; also $OsO_2(OEP)$ (**5**) was insoluble in common glass forming solvents and was studied in acetone. $Os(OEP)N_2(THF)$ was studied in the solution of THF and hydrazine hydrate in which the compound is generated from **5**.[11]

All ten Ru and Os complexes (Table I) were examined for emission in undegassed solutions at room temperature (300 K) and in liquid nitrogen (77 K). We covered the spectral range between 600 and 850 nm. In no case did we observe emission from undegassed samples at room temperature. Six of the complexes showed no emission at all, and we conclude that any quantum yield is below ca. $10^{-4}$. We also studied Ru(OEP)CO(py), Os(OEP)NO(OMe), $Os(OEP)N_2(THF)$, and $OsO_2(OEP)$ in deoxygenated solutions at room temperature. These solutions were prepared by bubbling argon deep into the solution through the fine capillary ending of a glass dropper for about 15 min. Then the absorption cell (SCC brand) was capped tightly, while bubbling argon close to the surface of the solution. Solutions deoxygenated in this way maintained constant emission over several hours at room temperature. We observed phosphorescence of Ru(OEP)CO(py) at room temperature in deoxygenated solutions both of 3-methylpentane and of EPA; similarly, we sbserved emission of $OsO_2(OEP)$ both in acetone and in benzene; however, similar preparations of Os(OEP)NO(OMe) both in EPA and in acetone and of $Os(OEP)N_2(THF)$ in THF showed no observable emission.

Quantum yields for the four complexes that showed emission, **2b**, **3b**, **3c**, and **5**, were estimated relative to Zn(Etio-I), whose fluorescence yield is $\phi_f = 0.04$ both at room and low temperature.[15-17] The yield studies of **2b**, **3b**, and **3c** were done vs. Zn(Etio-I), all in EPA at 77 K. The yield of **5** was determined in a degassed solution vs. Zn(Etio-I), both in benzene at room temperature. Yield estimates were based on the following numbers: (1) The intensity of the exciting source at the exciting wavelength had been previously determined using a radiometer.[18] (2) The optical density (OD) of the standard and the unknown were determined on a Cary 14; dilute solutions with OD in the range 0.10–0.16 were used except for one run on **3b**, which was studied with OD = 0.46 to enhance its very weak emission. (3) The intensity of emission was estimated by measuring the area of the uncorrected emission spectrum and multiplying by the detector sensitivity at the mean wavelength. Factors (1), (2), and (3) can be

**Table II.** $^1H$ NMR Data of the Complexes **2a–c** and **3a**[c]

| No. | Complex | Solvent (concn, mg/mL) | Porphyrin protons[a] t | q | s | Axial ligands[b] |
|---|---|---|---|---|---|---|
| **2a** | $Ru(OEP)py_2$ | $C_6D_6$ (25.0) | 1.79 | 3.72 | 9.39 | 2.04 |
| **2b** | Ru(OEP)CO(py) | $C_6D_6$ (25.0) | 1.81 | 3.81 | 9.93 | 1.20 |
| **2c** | Ru(OEP)NO(OMe) | $CDCl_3$ (28.0) | 2.01 | 4.41 | 10.22 | −2.69 |
| **3a** | $Os(OEP)py_2$ | $C_6D_6$ (25.0) | 1.73 | 3.59 | 8.48 | 3.10 |

[a] t, q, triplet and quartet of the ethyl groups; s, singlet of the protons at the methene bridges. [b] Only the upfield multiplet of the pyridine ligand is given since it should be the most sensitive to perturbations of the porphyrin $\pi$ system. For the nitrosyl compounds, this value represents the singlet arising from the $OCH_3$ group trans to NO. [c] $\delta$ in parts per million downfield from $Me_4Si$. JEOL JNM-C-60-HL and JNM-PS-100.

**Table III.** Iterative Extended Hückel Parameters[a]

| Metal | Ionization energies, eV | | | | Exponents, $au^{-1}$ [b] |
|---|---|---|---|---|---|
| Ru | $I_p = 7.36$ | | $I_p = 16.76$ | | |
| | $d^7s \rightarrow d^7 + (s)$<br>$d^6s^2 \rightarrow d^6s + (s)$<br>$d^6sp \rightarrow d^6p + (s)$ | 7.49 | $d^6s \rightarrow d^6 + (s)$<br>$d^5s^2 \rightarrow d^5s + (s)$<br>$d^5sp \rightarrow d^5p + (s)$ | 16.02 | s: 1.55 |
| | $d^7sp \rightarrow d^7 + (p)$<br>$d^6sp \rightarrow d^6s + (p)$ | 4.29 | $d^6p \rightarrow d^6 + (p)$<br>$d^5sp \rightarrow d^5s + (p)$ | 10.58 | p: 1.55 |
| | $d^8 \rightarrow d^7 + (d)$<br>$d^7s \rightarrow d^6s + (d)$<br>$d^7p \rightarrow d^6p + (d)$ | 8.88[c] | $d^7 \rightarrow d^6 + (d)$<br>$d^6s \rightarrow d^5s + (d)$<br>$d^6p \rightarrow d^5p + (d)$<br>$d^6s \rightarrow d^5s + (d)$ | 20.18 | d: 2.80 |
| Os | $I_p = 8.7$ | | $I_p = ?$ | | |
| | $d^6s^2 \rightarrow d^6s + (s)$<br>$d^6sp \rightarrow d^6p + (s)$ | 9.03 | $[\ ]s \rightarrow [\ ] + (s)$ | 16.19[d] | s: 1.81 |
| | $d^6sp \rightarrow d^6s + (p)$ | 5.82 | $[\ ]p \rightarrow [\ ] + (p)$ | 9.76[d] | p: 1.81 |
| | $d^7s \rightarrow d^6s + (d)$ | 8.1 | $[\ ]d \rightarrow [\ ] + (d)$ | 20.33[d] | d: 3.10 |

[a] Based on energy levels reported in ref 23. [b] Exponents used for iron: 1.38 (s); 1.38 (p); 3.06 (d). [c] Another extrapolation method gave 9.38 for this value; complexes **2a–c** were run with this value too with much the same results. [d] Another set of values [17.26 (s), 12.11 (p), 19.4 (d)] was extrapolated by another method, but gave similar results in several tests.

combined to determine quantum yield in the expected manner.[15] For **2b** and **3c**, our precision on several quantum yield determinations was within ±15%; however, the crudeness of our method suggests that the reported yield values should be considered valid only within ±30%. For **3b** and **5** we had larger precision errors, and these yields should be considered valid only within ±50%.

The apparatus for the determination of lifetimes has also been described previously.[15] The lifetime of the strobotac flash sets a lower limit to the lifetime we can measure as ≥6 μs.

**Iterative Extended Hückel (IEH) Method (A.A. and M.G.).** The iterative extended Hückel method and the program used have been previously reported along with parameters for H, C, N, O, and P.[19-21] The ionization potentials used for iron were also given earlier.[19] However, the basis set exponentials for the metals (Table **III**) were obtained by the method of Cusachs et al.[22] The exponentials for s and p orbitals were taken to be $[(n + 1/2)/\langle r \rangle]$ and for d orbitals $[(n + 1/2)(n + 1)/\langle r^2 \rangle]^{1/2}$ where $n$ is the principal quantum number and $\langle r \rangle$, $\langle r \rangle^2$ are atomic values obtained from SCF calculations.[22] Although these exponents are slightly different from those used in earlier work,[19] comparison runs on Fe, Co, and Ni gave no significant differences. The ionization energies for Ru and Os (Table **III**) were calculated in the same manner as before,[19] based on the spectroscopic tables of Moore.[23] (For details, see McGlynn et al.[24])

The geometry of the planar porphine ring was the same as that used previously,[19] except for displacement of the N atoms in accord with metal–nitrogen bond distance estimates. Metals were placed in the porphine ring plane. Crystal structures of Fe and Ru porphyrins have been studied.[25,26] The Os to ring nitrogen distance was taken the same as for Ru, since they both have the same covalent radii.[27] Metal to ligand bond lengths and angles involving the fifth and sixth ligands have been approximated from structure studies of similar compounds having the same oxidation state. These various bond lengths and angles are listed in Table IV.

The orientation of the porphyrin molecules with respect to coordinate axes was such that the center of the coordinate system coincided with the center of the porphyrin plane and the nitrogens of the ring were on the $x, y$ axes. The orientation of the ligands was chosen so as to maximize the number of symmetry planes for economy in computation time. Pyridine and THF were taken to be planar rings in the $xz$ plane, keeping the bond distances and angles as close as possible to x-ray values. For the methoxy groups, the M–O–C (M = metal) bond angle was taken as 120° with the three atoms located in the $xz$ plane; the hydrogens were in tetrahedral positions around the O–C bond; one of the hydrogens was in the $xz$ plane, thus preserving the $xz$ symmetry plane; the hydrogen in the $xz$ plane was located distal from the porphyrin ring. For $Os(P)[P(OMe)_3]_2$ the three oxygen atoms were in tetrahedral positions; one OC bond was located in the $xz$ plane; the other two OC bonds were parallel to the porphyrin plane; the methyl groups were tetrahedral and placed so as to avoid close approaches; the entire molecule had two planes of symmetry. It has been shown by various IEH calculations done at the University of Washington that rotation of the ligands with respect to the porphyrin plane does not affect the energy levels greatly, nor do the small variations in bond length shown in Table IV.

**Table IV.** Key Bond Lengths and Angles[b]

| Metal | | | Ligand | |
|---|---|---|---|---|
| | Length, Å | (angle) | | Length, Å |
| Fe–$N_p$ | 2.004 | | C–O | 1.14–1.16 |
| Fe–$N_{py}$ | 1.95 | | N–O | 1.13 |
| Fe–CO | 1.75 | (linear) | O–$CH_3$ | 1.42–1.44 |
| Ru–$N_p$[a] | 2.049 | | CH | 1.09 |
| Ru–$N_{py}$[a] | 2.10 | | N–N | 1.16 |
| Ru–CO[a] | 1.77 | (linear) | THF | C–C 1.56, 1.49 (2) |
| Ru–NO[a] | 1.78–1.80 | (linear) | | C–O 1.42 |
| Ru–OMe[a] | 2.00 | (120°) | | C–H 1.08 |
| Os–$P(OMe)_3$ | 2.41 | (tetrahedral) | | ∠COC 110° |
| Os–O | 1.80 | | | ∠CCC 100° |
| Os–$N_2$ | 2.00 | (linear) | py | C–C 1.40 |
| Os–O(THF) | 2.00 | | | C–H 1.08 |
| Os–F | 1.97 | | | C–N 1.34 |

[a] Same for Os. [b] $N_p$, porphyrin; $N_{py}$, pyridine; THF, tetrahydrofuran.

## Results and Discussion

**Constitution of the Compounds.** The constitution of most of the compounds under investigation has been corroborated elsewhere.[8-11,28] Additional evidence from elemental analysis, mass spectra, and NMR was reported above. Further support comes from parallel IR data between homologous Fe, Ru, and Os porphyrins. Thus the IR spectrum of the new $Ru^{II}$ nitrosonium methoxide, **2c**, shows the following bands characteristic for the axial ligands: 2775, 1055 ($\nu_{CH}$, $\nu_{CO}$ of the methoxide ligand), 1780 ($\nu_{NO}$ of the nitrosonium ion), and 491 $cm^{-1}$ ($\nu_{RuO}$ of the methoxide ligand). The corresponding values of the $Os^{II}$ analogue, **3c**, appear at 2780, 1065, 1745, and 497 $cm^{-1}$,[9] the lower NO-stretching frequency indicating stronger back-bonding in this compound as compared with **2c**.

Special care has been devoted to the identification of the bis(pyridine) complexes, **2a** and **3a**, because of the difficulties encountered in the interpretation of the IEH calculations discussed below. In addition to support from a crystal structure,[28] we prepared a large variety of bis(nitrogen base) complexes $Os(OEP)L_2$, where L = γ-picoline, MeCN, $NMe_3$,

$NHMe_2$, $NH_2Me$, or $NH_3$. The spectral and electrochemical data on these complexes fully correspond to the electron donor-acceptor balance expected for these ligands.[29] The typical IR vibrations for coordinated pyridine are found in **2a** at 1580, 1448, and 1268 $cm^{-1}$ and in **3a** at 1590, 1440, and 1270 $cm^{-1}$. Especially noteworthy are the large upfield shifts of the mesoprotons of the porphyrin ring in the $^1H$ NMR spectra of **2a** and **3a** (Table II); they indicate a high charge density on the porphyrin ring which is also evidenced by the IEH calculations (see below).

**Review of Porphyrin Electronic Spectra.** Before presenting the particular results on the absorption and emission spectra of Ru and Os complexes, it is useful to summarize the general classification scheme recently developed by two of the authors for porphyrin spectra,[6,7] because the Ru and Os spectra provide variations on the categories previously described.

Optical spectra of porphyrins fall into three absorption types (*normal, hypso,* and *hyper*); diamagnetic complexes have three emission types (*fluorescent, phosphorescent,* and *radiationless*).[7]

*Regular* porphyrins are found for metals from groups 1 to 5 in valence 1 to V, respectively. They have *normal* absorption; i.e., in the region $\lambda > 320$ nm they show only bands $N(\pi,\pi^*)$, $B(\pi,\pi^*)$, and $Q(\pi,\pi^*)$. The Q(0,0) (or $\alpha$) band occurs at $\lambda >$ 570 nm[30] for *normal* complexes M(OEP)LL′. These complexes are *fluorescent,* i.e., they show fluorescence yields $\phi_f > 10^{-3}$, as modified by the heavy atom effect.[7] Recent studies report regular complexes with metals from groups 4A,[31] 5A,[18,21,32] 4B,[15] and 5B.[15] The $Q(\pi,\pi^*)$ and $B(\pi,\pi^*)$ absorption as well as the fluorescence and phosphorescence are qualitatively interpreted in terms of the "four orbital" model,[33] and the spectra are more quantitatively described by $\pi$ electron theory.[34,35]

*Hypso* porphyrin spectra are like *normal* spectra but the $Q(\pi,\pi^*)$ bands are blue shifted to $\lambda < 570$ nm[30] for complexes M(OEP)LL′.[6,7] These spectra are usually found with transition metals with configurations $d^6$ to $d^9$ having $e_g(d_\pi)$ filled. Such complexes are either *phosphorescent* or *radiationless. Phosphorescent* complexes show very little fluorescence ($\phi_f < 10^{-3}$) but clear phosphorescence; examples are $Pd^{II}$, $Pt^{II}$,[36] and $Rh^{III}$.[37] Radiationless complexes have emission quantum yields below $10^{-4}$; examples are Co and Ni complexes[36] and iron complexes.[38]

The optical spectra of *hypso* complexes can be rationalized qualitatively as shown in Figure 1 for $d^6$. The main factors at play are (1) the ligand field splitting $\Delta$ between the filled orbitals $(d_{xy})^2(d_\pi)^4$ and the empty orbitals $d_{z^2}$, $d_{x^2-y^2}$; (2) the energy for charge transfer (CT) transitions from metal to ring; and (3) the mixing of filled $e_g(d_\pi)$ and empty $e_g(\pi^*)$ orbitals (back-bonding), indicated by $\lambda$ in Figure 1. (1) When the gap $\Delta$ is small, as with first-row transition metals, low-lying (d,d) transitions may intervene between the lowest $(\pi,\pi^*)$ level and the ground state causing the complexes to be radiationless.[38,39] (2) Charge transfer transitions $e_g(d_\pi) \rightarrow e_g(\pi^*)$ can also be expected to provide low-energy transitions that can cause the compounds to be radiationless. (3) Finally the mixing of $e_g(\pi^*)$ and $e_g(d_\pi)$ orbitals (i.e., back-bonding) indicated by $\lambda$ in Figure 1 has two effects: (a) the levels $e_g(\pi^*)$ are pushed to higher energy giving rise to the hypsochromic effect; and (b) the parameter $\lambda$ produces a strong spin-orbit coupling that decreases triplet lifetime.

*Hyper* porphyrin spectra, in the region $\lambda > 320$ nm, show other intense absorption ($\epsilon > 1000$ $M^{-1}$ $cm^{-1}$) in addition to $N(\pi,\pi^*)$, $B(\pi,\pi^*)$, and $Q(\pi,\pi^*)$ bands. Two types of *hyper* spectra are fairly well understood:[6,7] *p-type hyper* spectra are found in $Sn^{II}$, $Pb^{II}$, $P^{III}$, $As^{III}$, $Sb^{III}$, and $Bi^{III}$ porphyrins, where the extra bands are of $a_{2u}(np_z) \rightarrow e_g(\pi^*)$ character (i.e., metal $\rightarrow$ ring charge transfer);[18,20,21,31] *d-type hyper* spectra are found with transition metal complexes, e.g., $Fe^{III}$, $Mn^{III}$, $Cr^{III}$, $Mo^V$, and $W^V$, that have vacancies in the $e_g(d_\pi)$ orbitals and have low metal redox potentials; in these cases the extra bands are of $a_{1u}(\pi)$,$a_{2u}(\pi) \rightarrow e_g(d_\pi)$ character (i.e., ring $\rightarrow$ metal charge transfer).[7]

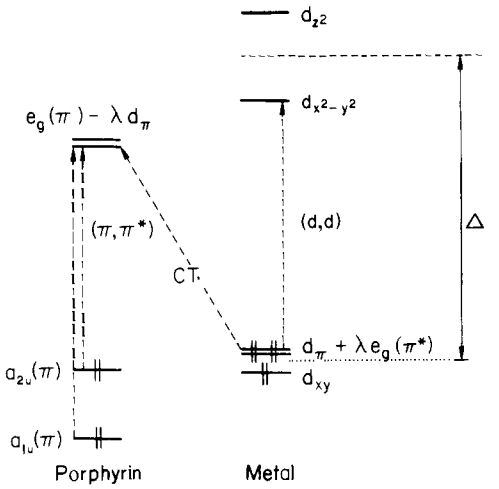


**Figure 1.** Schematic illustration of important orbitals for the spectra of $d^6$ six-coordinate porphyrins: (1) $\Delta$, the ligand field gap determining (d,d) transitions; (2) charge transfer transitions, $(d,\pi^*)$; (3) the back-bonding parameter, $\lambda$, determining hypsochromic effect and spin-orbit coupling.

**Optical Absorption Studies.** Table V reports peak optical absorption data taken in Aachen including log $\epsilon$ ($\epsilon$ the molar extinction coefficient). The spectra shown in Figures 2-6 were taken in Seattle, Wash., using the solvents in which the emissions were studied.

Ru(OEP)CO(py) (**2b**) would seem to show a typical *hypso* absorption spectrum, showing blue-shifted Q bands and a very intense, sharp B (Soret) band (Figure 2). [The weak band with $\lambda \sim 595$ nm (Figure 2) has been shown to belong to an impurity by phosphorescence excitation spectra.] However, the prominent tail to the red of the Soret band, verified by phosphorescence excitation spectra, shows evidence of other than $(\pi,\pi^*)$ transitions in the visible region. We therefore classify this compound as *hypso/hyper.* Note also that the spacing between Q(1,0) and Q(0,0) is 1090 $cm^{-1}$, substantantially smaller than the customary value of ~1250 $cm^{-1}$. The absorption spectrum of Os(OEP)CO(py) (**3b**), also shown in Figure 2, is quite similar to that of **2b;** however, the Q bands are more blue shifted and are anomalously broadened. This broadening is evidence for weak underlying bands. Thus **3b** is also classified as *hypso/hyper.*

The absorption spectrum of Os(OEP)NO(OMe) (**3c**), shown in Figure 3, would also seem to be typically *hypso.* However, the Soret band is anomalously broadened, and the ratio $\epsilon_{max}(B)/\epsilon_{max}(Q)$ is lower than that of either **2b** or **3b** shown in Figure 2. There is a somewhat more prominent absorption band at $\lambda \sim 345$ nm than is shown by **2b** and **3b.** Thus we characterize this spectrum as *hypso/hyper.* The spectrum of Ru(OEP)NO(OMe) (**2c**) is more clearly *hyper,* having a pronounced shoulder to the red of the Soret band and a tail to the red of Q(0,0). Since Q(0,0) is blue shifted, it too is *hypso/hyper.*

In Figure 4, the two bispyridine complexes, **2a** and **3a,** give very clear examples of *hypso/hyper* spectra. The Q bands are very prominent as well as very blue shifted. The ratio $\epsilon_{max}(B)/\epsilon_{max}(Q)$ is anomalously low compared to *normal* metalloporphyrins, and there are several prominent absorption bands between the Soret and Q bands. Moreover, Ru(OEP)$py_2$ shows a tail to the red of Q(0,0) and Os(OEP)$py_2$ shows a clear peak at $\lambda \sim 597$ nm.

Figure 5 gives the spectrum of two other $Os^{II}$ species:

**Table V.** Electronic Absorption Maxima (nm) with Extinction Coefficients (log $\epsilon$)[a] of the Complexes **2a–c**, **3a–e**, **4**, and **5**

| No. | Complex | Solvent | Other | Soret \|B(0,0)\| | Other | $\beta$ \|Q(1,0)\| | $\alpha$ \|Q(0,0)\| |
|---|---|---|---|---|---|---|---|
| **2a** | $Ru(OEP)py_2$ | $C_6H_6$ | *b* | 395 (5.01) | 450 (4.20) | 495 (4.17) | 521 (4.58) |
| **3a** | $Os(OEP)py_2$ | $C_5H_5N$ | *c* | 389 (5.04) | 410 (4.59) | 482 (4.36) | 510 (4.71) |
| **2b** | Ru(OEP)CO(py) | $CH_2Cl_2$ | | 396 (5.37) | | 518 (4.20) | 549 (4.39) |
| **3b** | Os(OEP)CO(py) | $CH_2Cl_2$ | 350 (4.32) | 394 (5.48) | | 510 (4.11) | 540 (4.31) |
| **2c** | Ru(OEP)NO(OMe) | $CH_2Cl_2$ | 345 (4.48) | 392 (5.08) | | 539 (4.08) | 572 (4.12) |
| **3c** | Os(OEP)NO(OMe) | $CH_2Cl_2$/ $CH_3OH$ | 342 (4.56) | 419 (4.96) | | 533 (4.23) | 568 (4.44) |
| **3d** | $Os(OEP)[P(OMe)_3]_2$ | $CH_2Cl_2$ | 348 (4.49) | 406 (5.25) | | 500 (4.10) | 522 (4.21) |
| **3e** | $Os(OEP)N_2(THF)$[d] | THF | | 393 (5.18) | | 498 (4.15) | 523 (4.30) |
| **4** | $Os(OEP)(OMe)_2$ | $CH_2Cl_2$/ $CH_3OH$ | | 370 (5.09) | | 497 (3.97) | 530 (3.90) |
| **5** | $OsO_2(OEP)$ | $CH_2Cl_2$ | | 378 (5.09) | 428 (4.26) | 470[e] (4.18) | 578[e] (3.95) |

[a] Recorded at room temperature (Unicam SP 800B). [b] Weak near-IR bands observed at ~645 sh, ~715 sh nm. [c] Weak near-IR bands observed (in $C_6H_6$) at 648 sh, 723 sh, 850 broad, 980 broad nm. See Figure 4. [d] Values measured indirectly by reaction of hydrazine hydrate with **5** in the spectroscopic solution; absorption intensity values of the product were recorded when the bands of the starting material had disappeared. [e] Because of charge transfer transitions, these peaks are not assigned as $\alpha$ and $\beta$ bands. See text.

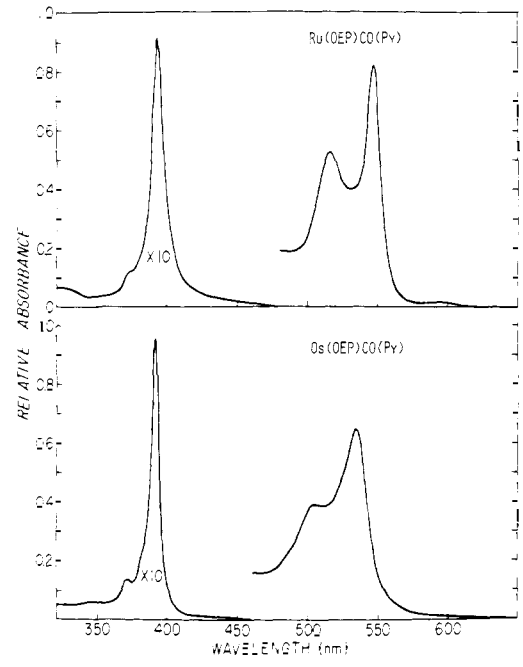


**Figure 2.** Absorption spectra of Ru(OEP)CO(py) (**2b**) and Os(OEP)-CO(py) (**3b**) at room temperature in 3-methylpentane. Possible charge transfer bands (d,$\pi^*$) identified as the tail absorption ~440 nm in **2b** and underlying the Q($\pi,\pi^*$) bands ~540 nm in **3b**, causing their broadness.

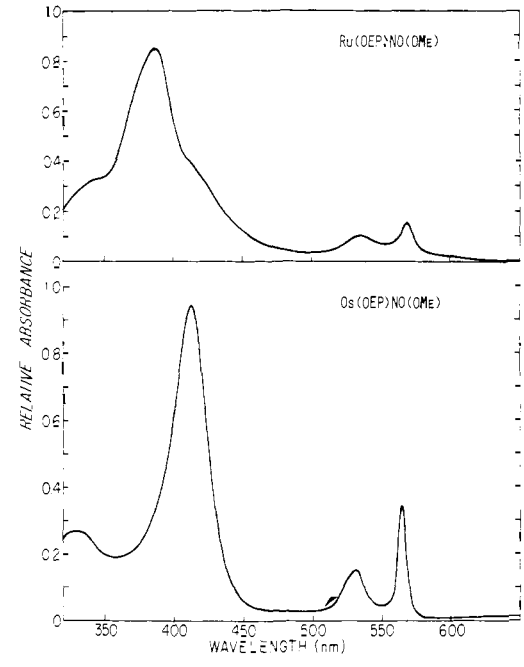


**Figure 3.** Absorption spectra of Ru(OEP)NO(OMe) (**2c**) and Os(OEP)-NO(OMe) (**3c**) at room temperature in 3-methylpentane. Possible charge transfer bands, $a_{1u}(\pi)$, $a_{2u}(\pi) \rightarrow [NO(\pi^*) + e_g(d_\pi)]$ identified as the shoulder ~410 nm in **2c** and the band ~330 nm in **3c**.

$Os(OEP)[P(OMe)_3]_2$ and $Os(OEP)N_2(THF)$. Both are basically *hypso*. The Soret bands are sharp, and the ratio of Soret to visible absorbance maxima is relatively *normal*. However, the Q bands are quite broadened and have marked tails to the red, suggesting possible extra underlying forbidden transitions. Thus, all the $Ru^{II}$ and $Os^{II}$ spectra are classified as *hypso/hyper*.

Figure 6 shows the absorption of the $Os^{IV}$ and $Os^{VI}$ complexes **4** and **5**. Both are clearly *hyper*. The Soret bands of both compounds, though quite intense with respect to the visible bands, are anomalously broad. The Q bands for Os(OEP)-$(OMe)_2$ are anomalous in appearance, and the compound has a broad red band at $\lambda$ ~610 nm. The spectrum of $OsO_2(OEP)$ follows that typical of *d-type hyper* complexes with three distinct band systems at ~370, ~450, and ~580 nm. All three bands are broad but structured. Both **4** and **5** have holes in the $e_g(d_\pi)$ shell, so the *d-type hyper* spectra are not unexpected.

As to the relations among these spectra, we might note that $\lambda$(Q) decreases along the series M(OEP)NO(OMe) > M(OEP)CO(py) > $M(OEP)py_2$ for both M = Ru and Os. For M(OEP)LL′, with L and L′ fixed, $\lambda$(Q) decreases along the series Fe > Ru > Os. However, $\lambda$(B) show no similar systematic shifts.

**Optical Emission Studies.** The emission spectra of four

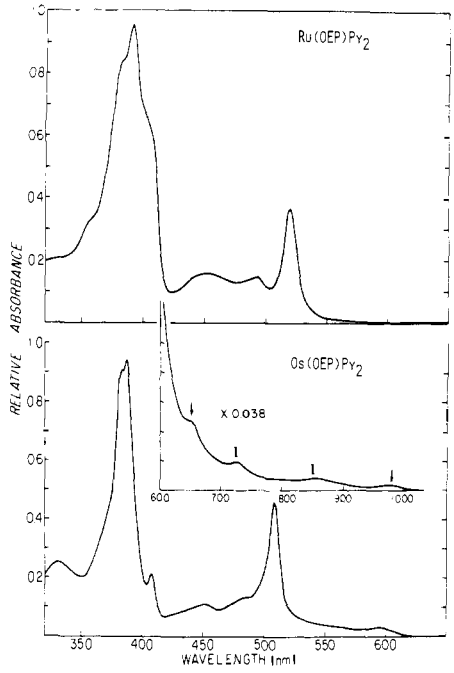


**Figure 4.** Absorption spectra of $Ru(OEP)py_2$ (**2a**) and $Os(OEP)py_2$ (**3a**) at room temperature in 3-methylpentane. The many extra bands are attributed to doubly excited states $[e_g(d_\pi)]^3[a_{1u}a_{2u}]^3[e_g(\pi^*)]^2$. The near-IR absorption [inset for $Os(OEP)py_2$] should be multiplied by 0.038 to compare to visible-UV spectrum; arrows show peaks (Table V, footnote *c*), attributed to charge transfer ($d,\pi^*$) excited states.

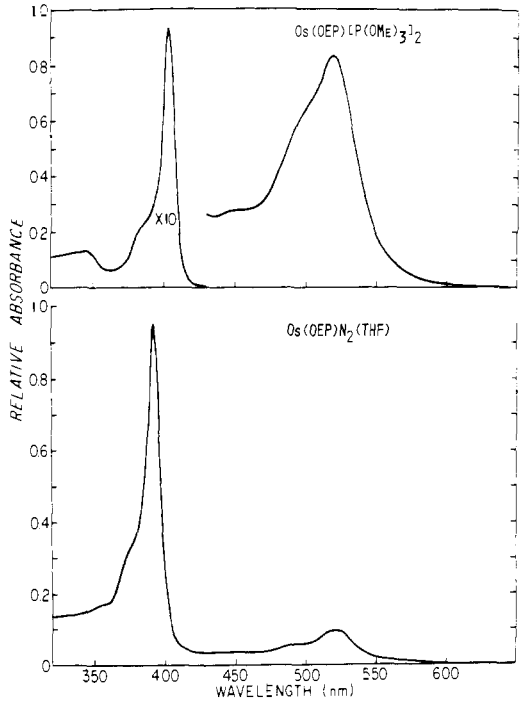


**Figure 5.** Absorption spectra of $Os(OEP)[P(OMe)_3]_2$ (**3d**) and $Os(OEP)N_2(THF)$ (**3e**) at room temperature in 3-methylpentane and tetrahydrofuran, respectively. The broadness of the $Q(\pi,\pi^*)$ bands is attributed to underlying charge transfer ($d,\pi^*$) transitions.

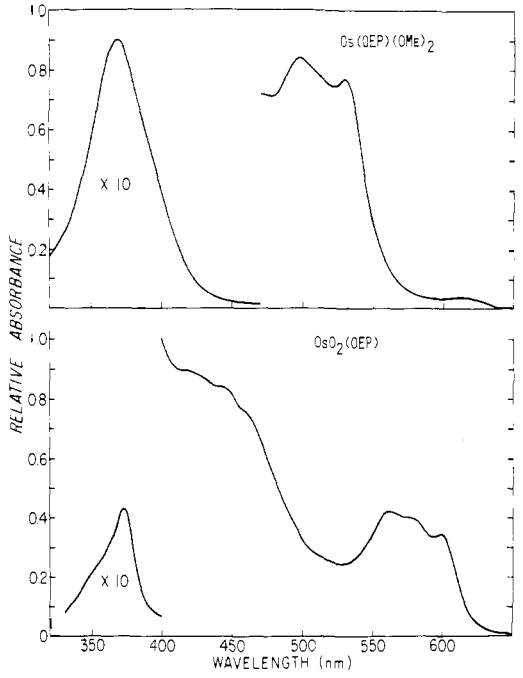


**Figure 6.** Absorption spectra of $Os(OEP)(OMe)_2$ (**4**) and $OsO_2(OEP)$ (**5**) at room temperature in EPA and acetone, respectively. The extra bands are attributed to charge transfer ($\pi,d_\pi$) transitions.

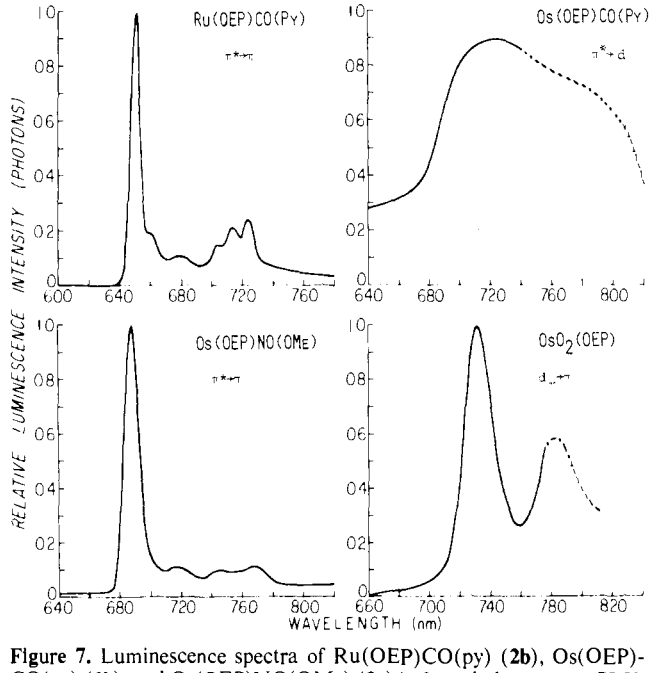


**Figure 7.** Luminescence spectra of Ru(OEP)CO(py) (**2b**), Os(OEP)-CO(py) (**3b**), and Os(OEP)NO(OMe) (**3c**) in 3-methylpentane at 77 K; luminescence spectrum of $OsO_2(OEP)$ (**5**) in degassed acetone solution at room temperature. All spectra were corrected for the variation of detector sensitivity with wavelength. Dashed regions indicate uncertainty due to excessive noise; note the nonzero baseline of **3b**. The emissions of **2b** and **3c** are from ring $T_1(\pi,\pi^*)$ excited states. The emission of **3b** is attributed to a $T(d,\pi^*)$ excited state and that of **5** to an excited state with substantial $T(\pi,d_\pi)$ character.

complexes are shown in Figure 7. In Table VI we have given the principal emission peaks, the quantum yield estimates, and the measured lifetimes.

Two compounds, Ru(OEP)CO(py) and Os(OEP)-NO(OMe), show phosphorescence bands with sharp origins, at 653 and 688 nm, respectively, followed by several substantially weaker vibronic bands. These phosphorescence spectra are rather like those shown by etioporphyrin complexes of $Pd^{II}$, $Pt^{II}$,[36] and $Rh^{III}$ [37] and can be identified as emission from the $T_1(\pi,\pi^*)$ excited state. The emission decay of Ru(OEP)-CO(py) is exponential at 77 K with a lifetime of 405 $\mu$s. This is comparable to but shorter than the decay times observed for etioporphyrin complexes of $Pd^{II}$ (1930 $\mu$s)[36] and $Rh^{III}$ (730 $\mu$s).[37] The emission of Os(OEP)NO(OMe) at 77 K shows a nonexponential decay, that could be fit as a sum of two expo-

**Table VI.** Emission Maxima, Relative Quantum Yields, and Lifetimes

| No. | Compd | Solvent[a] | Phosphorescence peaks, nm | | | | | | Quantum yield[c] | Lifetime, μs | Temp, K |
|---|---|---|---|---|---|---|---|---|---|---|---|
| **2b** | Ru(OEP)CO(py) | 3MP | 653[b] | 661 | 681 | 704 | 714 | 725 | $6 \times 10^{-2}$ | 405 | 77 |
| **3b** | Os(OEP)CO(py) | 3MP | ~720 | ~782 | | | | | $6 \times 10^{-4}$ | <6 | 77 |
| **3c** | Os(OEP)NO(OMe) | 3MP | 688[b] | 718 | 746 | 769 | | | $3 \times 10^{-3}$ | 116/35 | 77 |
| **5** | $OsO_2$(OEP) | Acetone | 729[b] | 781 | | | | | $5 \times 10^{-3}$ | <6 | ~300 |

[a] See footnotes to Table I for abbreviations. [b] Clear (0-0) origin. [c] Rough estimate. See text for accuracy.

nential decays with lifetimes of 116 and 35 μs. This compares to the exponential phosphorescence decay of Pt(Etio) with a lifetime of 121 μs.[36] The phosphorescence quantum yields of these Ru and Os complexes are substantially lower than the yields observed for the etioporphyrin complexes of $Pd^{II}$ (0.5),[36] $Rh^{III}$ (0.23),[37] and $Pt^{II}$ (0.9).[36]

Although Hopf et al.[28] reported delayed fluorescence at λ 556 nm from Ru(OEP)CO(py), we saw only $T_1(\pi,\pi^*)$ phosphorescence in deoxygenated solution at room temperature. Similar preparations of Os(OEP)NO(OMe) in deoxygenated solution at room temperature showed no observable emission. This suggests that the latter compound has a state above $T_1(\pi,\pi^*)$ that is thermally populated at room temperature and that has fast radiationless decay to the ground state.

The emissions of Os(OEP)CO(py) and $OsO_2$(OEP) were both unusual. For Os(OEP)CO(py) the emission was very weak, very broad, and substantially red shifted from the emission of Ru(OEP)CO(py), even though the absorption of the Os complex is *blue* shifted from its Ru analogue. Moreover, we could not determine any lifetime above 6 μs. This anomalous emission suggests that the excited state is not the usual $^3T_1(\pi,\pi^*)$ state. The emission of $OsO_2$(OEP) is very red shifted from the $T_1(\pi,\pi^*)$ emission range. The room temperature lifetime is very short (<6 μs). Since there is no clear absorption mirror image to this peak, the emitting state is identified as a triplet. A similar emission to that reported in Figure 7 for **5** at room temperature was also observed in acetone snow at 77 K.[56]

**Interpretation of Electronic States by IEH Calculations.** The molecular orbital energy diagrams resulting from our calculations are given in Figures 8-12. In these figures the molecular orbitals have been grouped depending on whether the electron density is largest on the porphine ring (P), metal (M), or ligand (L). $D_{4h}$ symmetry labels are used for the porphyrin MOs, even in cases where ligands lower the symmetry. Although the calculations are done on the unsubstituted porphine ring, we do not expect the ethyl substituents to grossly affect metal-porphyrin-ligand interactions.

Charge densities are given in Table VII. We see that the py, THF, and $P(OMe)_3$ are positive, consistent with σ donor character. While (OMe) is negative, the charge is much smaller than expected for the formal charge of −1, so this ligand is also a σ donor. On the other hand, $N_2$, CO, and $NO^+$ are electron acceptors. We have analyzed the character of the low-energy π* orbitals on these ligands and conclude that π acceptor properties increase in the order py < $N_2$ < CO < $NO^+$. py has almost no π acceptor activity by the IEH calculations.

Before discussing the IEH calculations on particular molecules, it should be noted that the IEH orbital energy differences are an inaccurate guide to estimating excited state energies, particularly for charge transfer transitions. Basically this arises from using a one-electron model to explain excited states, which have substantial electron rearrangement from the ground state. A general argument has recently been given on why charge transfer transitions are generally higher (by ~1 eV) than the energy gap between orbitals calculated by the IEH model.[40] We might also note that nonbonding orbitals on

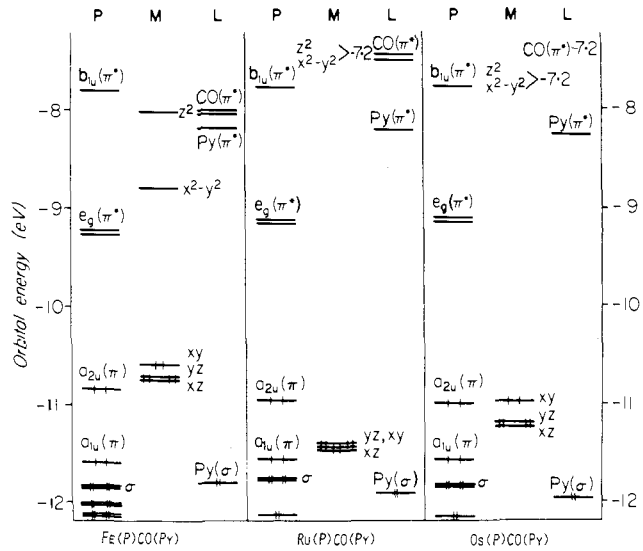


**Figure 8.** Energies of top filled and lowest empty MOs calculated by the iterative extended Hückel method. MOs are grouped as P, M, or L depending on whether the electron density for the MO is largely on the porphine ring (P), metal (M), or ligand (L); $D_{4h}$ symmetry labels.

OH ligands are calculated to have much too high energies,[20,21] so that CT transitions from such O(p) nonbonding orbitals to $e_g(\pi^*)$ are even more underestimated. [This appears to be true for the O(p) orbitals of Figures 9 and 10.]

Consider first the three carbonyl-pyridine complexes, **1b**, **2b**, and **3b**, whose orbitals are shown in Figure 8. **1b** is predicted to show low-energy (d,d) transitions; such transitions are indeed observed and act to quench emission from the Fe complex.[38,39] No such transitions are expected for **2b** and **3b**, and a strong phosphorescence from $T_1(\pi,\pi^*)$ is predicted. This is indeed observed for **2b**. However, **3b** is anomalous in absorption in having a broadened $Q(\pi,\pi^*)$ band; and its emission is unusual in being red shifted, broad, and very weak. Figure 8 suggests that both of these anomalies might be due to low-energy excited states of charge transfer $(d,\pi^*)$ origin, which are calculated to be at somewhat lower energy for **3b** than for **2b**. Thus the data suggest that the filled d orbitals for **3b** are at somewhat higher energy than shown in Figure 8.

Consider next the two nitrosonium methoxides **2c** and **3c** (Figure 9). The IEH model predicts allowed CT transitions to the empty orbitals of mixed $[NO(\pi^*) + e_g(d_\pi)]$ character. Thus the *hyper* character of the spectra is explained. Presumably new transitions of character $a_{1u}(\pi)$, $a_{2u}(\pi) \rightarrow [NO(\pi^*) + e_g(d_\pi)]$ are responsible for the absorption of **2c** at about 410 nm. Figure 9 suggests that these transitions are at higher energy in **3c** than in **2c**. The absorption data of Figure 3 are in agreement with this result. Note that in both compounds the filled d orbitals are pushed down to low energy, presumably owing to back-bonding to the empty $NO(\pi^*)$ orbitals. The reason for the lack of emission from the Ru species compared to the strong emission from the Os is not so clear. Possibly the presence of more CT character in the low-energy excited states acts to quench emission. We have shown calcu-

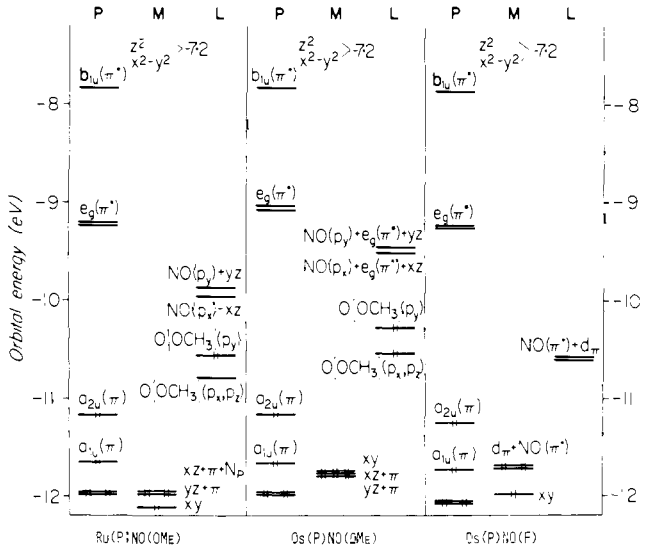


Figure 9. See legend with Figure 8.

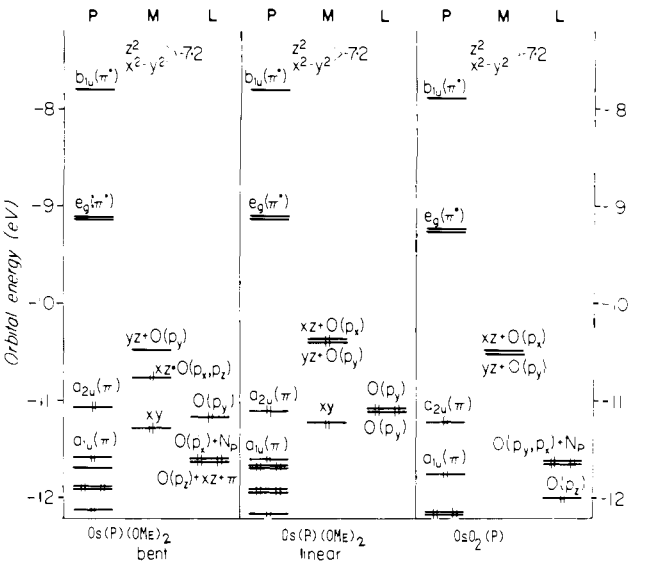


Figure 11. See legend with Figure 8.

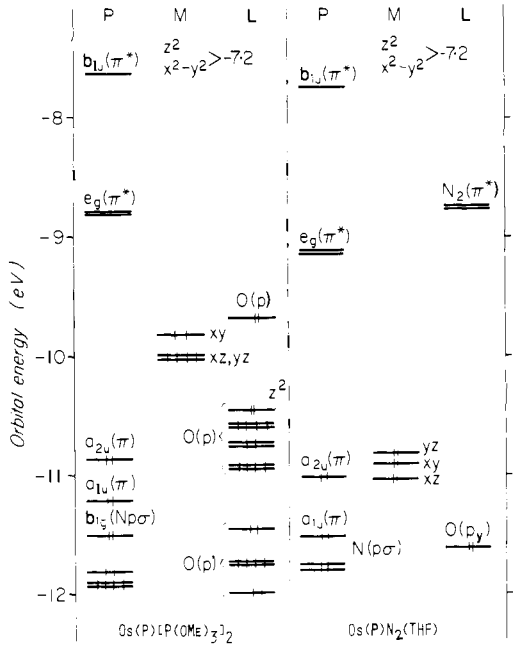


Figure 10. See legend with Figure 8.

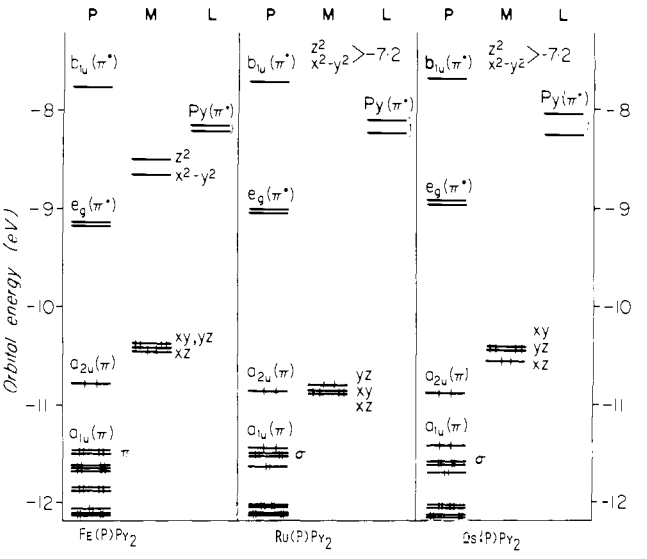


Figure 12. See legend with Figure 8.

lations on Os(OEP)NO(F) in Figure 9. It lacks O(p) orbitals from the OMe group, which appear at anomalously high energy, as mentioned above;[20,21] however, its absorption spectrum is nearly identical with that of Os(OEP)NO(OMe), and it also shows similar emission.[41,42] (Parameters for the fluoride calculation will be given elsewhere.[42])

$Os(OEP)[P(OMe)_3]_2$ (**3d**) and $Os(OEP)N_2(THF)$ (**3e**) show in their optical absorption (Figure 5) a broadness of the visible region. Neither shows emission. For **3d,** Figure 10 predicts low-energy forbidden (d,$\pi^*$) transitions that could broaden the visible absorption and quench emission. For $Os(OEP)N_2(THF)$, the d orbitals are calculated to be slightly higher than for Os(OEP)CO(py) (compare Figures 8 and 10). Therefore, in this compound also, low-energy forbidden (d,$\pi^*$) transitions may be broadening the visible band and quenching emission.

As expected, the calculations on $Os(OEP)(OMe)_2$ (**4**) and $OsO_2(OEP)$ (**5**) of Figure 11 show unfilled $e_g(d_\pi)$ orbitals, thus explaining their *hyper* character. For **4** the calculations show a half-filled $e_g(d_\pi)$ shell. For comparison we have shown the molecule calculated with the OMe groups both linear and bent. The linear orientation leads to a paramagnetic triplet ground state. The splitting of the $d_{xz}$, $d_{yz}$ orbitals depends on the amount of bending. Thus the bent molecule must have a very low energy triplet excited state. The existence of such a state is suggested by the observation of a temperature-independent paramagnetism over the range 77-300 K with an effective magnetic moment of 1.11 $\mu_B$.[41]

The *hyper* absorption of **5** (Figure 6) resembles that of other *hyper* species, e.g., containing $Mn^{III}$,[43] in having three band systems: ~370, ~450, and ~580 nm. This suggests a six-orbital model involving transitions $a_{1u}(\pi), a_{2u}(\pi) \rightarrow e_g(\pi^*)$, [$e_g(d_\pi)$ + $O(p_x,p_y)$]. All these transitions have $E_u$ symmetry and should be subject to mixing by configuration interaction. However, since the extra absorption band at 450 nm is rather weaker than a *normal* Soret band, we expect that it contains more charge transfer rather than ring ($\pi,\pi^*$) character. The substantial red shift of this emission band probably results from mixing between the normal ring $T_1(\pi,\pi^*)$ triplet states and charge transfer triplets of $T(\pi,d_\pi)$ character. Further study of this emission between 77 and 2 K may reveal large triplet sublevel splitting, such as has been found by Crosby and coworkers in the charge transfer emission of the tris(2,2′-bipy-

**Table VII.** Charge Densities[a]

| Compd $M(P)L_1L_2$ | Porphine (P) | Metal (M) | Ligand ($L_1$) | Ligand ($L_2$) | Total ligand | Symmetry |
|---|---|---|---|---|---|---|
| $Fe(P)py_2$ | −0.578 | 0.146 | 0.216 | 0.216 | 0.432 | $D_{2h}$ |
| Fe(P)CO(py) | −0.334 | 0.187 | −0.078 | 0.226 | 0.148 | $C_{2v}$ |
| $Ru(P)py_2$ | −0.685 | 0.214 | 0.236 | 0.236 | 0.472 | $D_{2h}$ |
| Ru(P)CO(py) | −0.344 | 0.271 | −0.167 | 0.240 | 0.073 | $C_{2v}$ |
| Ru(P)NO(OMe) | −0.112 | 0.340 | −0.098 | −0.131 | −0.229 | $C_s$ |
| $Os(P)py_2$ | −0.730 | 0.220 | 0.255 | 0.255 | 0.510 | $D_{2h}$ |
| $Os(P)CO(py)_2$ | −0.345 | 0.282 | −0.199 | 0.271 | 0.072 | $C_{2v}$ |
| Os(P)NO(OMe) | −0.104 | 0.358 | −0.147 | −0.107 | −0.254 | $C_s$ |
| $Os(P)[P(OMe)_3]_2$ | −0.969 | 0.172 | 0.399 | 0.399 | 0.798 | $C_{2v}$ |
| $Os(P)N_2(THF)$ | −0.450 | 0.271 | −0.122 | 0.299 | 0.177 | $C_{2v}$ |
| Os(P)NO(F) | 0.067 | 0.373 | −0.047 | −0.393 | −0.440 | $C_{4v}$ |
| $Os(P)(OMe)_2$ bent | −0.256 | 0.310 | −0.027 | −0.027 | −0.054 | $C_{2v}$ |
| $Os(P)(OMe)_2$ linear | −0.303 | 0.314 | −0.005 | −0.005 | −0.010 | $C_{2v}$ |
| $OsO_2(P)$[b] | 0.092 | 0.440 | −0.266 | −0.266 | −0.532 | $D_{4h}$ |

[a] Calculated for unsubstituted porphine ring. [b] Note: dioxo, not dioxygen.

ridine)ruthenium(II) cation and related complexes.[44,45]

A comparison of Figures 8 and 12 suggests that the bispyridine complexes, **1a, 2a,** and **3a,** should have rather similar spectra to the carbonyl-pyridine complexes, **1b, 2b,** and **3b,** except for more interference by forbidden $d \rightarrow e_g(\pi^*)$ transitions. Comparison of Figures 2 and 4 show very different absorption spectra for **2a** and **3a** compared to **2b** and **3b.** The extra bands of **2a** and **3a** in the visible region are very intense, suggesting that there are extra allowed transitions in the region. However, the orbital diagram of Figure 12 gives only one possible candidate for an extra allowed transition, i.e., $d \rightarrow py(\pi^*)$. However, this transition is calculated to be at rather high energy; moreover, it is similarly present in Figure 8. A final reason for rejecting this transition as a cause of the extra bands in **2a** and **3a** is the fact that the molecule $Os(OEP)(NH_3)_2$ has a rather similar absorption spectrum[41] to the complex **3a,** and $NH_3$ has no low-energy vacant orbitals. We also considered the possibility that the extra bands arise from an unusually intense vibronic coupling between the forbidden $(d,\pi^*)$ and the allowed $(\pi,\pi^*)$ transitions; however, this seems unlikely because it is difficult to construct a vibronic argument to explain why such strong couplings are present in **2a** and **3a** but are absent in **2b, 3b, 3d,** and **3e.**

The most plausible explanation that we can find for the extra absorption bands of the bispyridine complexes involves the presence of allowed doubly excited states in the visible region. This follows theoretical work of Kobayashi and co-workers, who developed an "extended circular box" model to explain the absorption spectra of various Co and Fe porphyrin spectra. In the original circular box model,[46] the top filled $\pi$ orbitals have angular momentum ±4 and the lowest empty $\pi^*$ orbitals have ±5. The ground state of porphyrin has electron configuration $(4)^4$ and the *normal* (see above) Q and B bands arise from excited configurations $(4)^35$. Kobayashi et al.[47-51] in treating Fe and Co complexes also included the $d_\pi$ orbitals with angular momentum ±1.

In the case of $Co^I$,[47] in addition to the ground state $(1)^4(4)^4$ and Q and B excited states $(1)^4(4)^35$, they considered the forbidden charge transfer excited states $(1)^3(4)^45$ and the doubly excited states $(1)^3(4)^3(5)^2$. The charge transfer states occur at 4000 $cm^{-1}$, and the doubly excited states provide eight pairs of $^1E_u$ states scattered over the region from 19 100 to 27 700 $cm^{-1}$. These couple by configuration interaction to the *normal* excited states $(1)^4(4)^35$ to provide an unusual *hyper* absorption spectrum for $Co^I$ complexes.[47]

Although the IEH model calculations of Figure 12 would not lead one to expect that the charge transfer states $(1)^3(4)^4(5)^2$ should occur in the visible-near-UV region, qualitative arguments suggest that this is not implausible. The electron densities (Table VII) show that the pyridine ligands are positive. While the IEH calculations show that most of this density is on the porphyrin ring rather than on the metal, if this is incorrect and most of the density is on the metal then the low energy of configurations $(1)^3(4)^45$ and $(1)^3(4)^3(5)^2$ becomes reasonable.

In an effort to substantiate this interpretation of the spectra of the bispyridine complexes, we carefully examined the absorption in the near IR to find evidence that forbidden CT transitions, $d \rightarrow e_g(\pi^*)$, are present in **2a** and **3a** but are absent in **2b** and **3b.** We studied absorption in concentrated benzene solutions of these four complexes between 600 and 1600 nm (6250 $cm^{-1}$), where strong benzene absorption occurs. No peaks or shoulders are apparent in **2b** and **3b.** However, **2**a and **3**a show clear shoulders (Table V, footnotes *b* and *c*), which were more apparent in **3a** (Figure 4).

Electrochemical studies by Brown et al.[52,53] provide further support for our interpretation of the optical spectra of Ru and Os porphyrin complexes. These workers found that the first oxidation waves of $Ru(TPP)py_2$ [TPP = tetraphenylporphine], of Ru(OEP)py(MeCN), and of Os(OEP)CO(py) with $E_{1/2}$ = 0.21, 0.08, and 0.48 V, respectively, correspond to metal oxidation; however, the first oxidation waves of Ru(TPP)CO(py) and of Ru(OEP)CO with $E_{1/2}$ = 0.81 and 0.64 V, respectively, correspond to ring oxidations. It has been noted that

$$\Delta E(\pi \rightarrow \pi^*) \sim E^{ox}_{1/2}(1) - E^{red}_{1/2}(1)$$

where $\Delta E(\pi,\pi^*)$ is the energy for the $\pi \rightarrow \pi^*$ absorption and $E^{ox}_{1/2}(1)$ and $E^{red}_{1/2}(1)$ are the half-cell potentials for the first ring oxidation and reduction.[54] It was later suggested that this relation might apply roughly to charge transfer transitions.[40] The redox studies of Brown et al.[52,53] would then be consistent with low-energy $(d,\pi^*)$ CT transitions in complexes $M(OEP)py_2$; with $(d,\pi^*)$ approximately comparable to $(\pi,\pi^*)$ transitions in Os(OEP)CO(py); but with $(d,\pi^*)$ at higher energy than $(\pi,\pi^*)$ in Ru(OEP)CO(py). Thus the optical studies reported here combined with earlier redox studies[52,53] substantiate the conjecture[40] that CT transition energies can be roughly estimated from redox potentials.

It is of some interest to ask whether the $(d,\pi^*)$ transitions we have identified in the complexes **2**a and **3a** are also present in the iron complex **1a;** similarly whether the doubly excited states identified in the bispyridine complexes **2b** and **3b** are present in **1b.** The spectra reported for **1**a and **1b**[5] and their similarity to those of the Ru and Os homologues suggest that similar transitions might be present. However, recent resonance Raman reported on **1b** suggests that the extra band at 472 nm is due to charge transfer to the pyridine.[55] Clearly

comparative resonance Raman studies among these complexes will be necessary to substantiate the identifications proposed here and determine their importance in heme complexes.

## Summary and Conclusion

In this paper we have reported on optical absorption and emission and IEH calculations on ten Ru and Os porphyrins, **2–5.** A wide variety of absorption and emission spectra are observed. Comparison of the spectra with IEH calculations leads to the following general view of extra low energy excited states of these systems not of $(\pi,\pi^*)$ origin: The $Os^{IV}$ and $Os^{VI}$, **4** and **5,** have vacancies in the $e_g(d_\pi)$ orbitals and have *hyper* absorption spectra due to low energy states of $(\pi,d_\pi)$ character; the emission of **5** is ascribed to a triplet state containing substantial $T(\pi,d_\pi)$ character. The $Ru^{II}$ and $Os^{II}$ complexes all show what we have called *hypso/hyper* absorption: The $Q(\pi,\pi^*)$ bands are blue shifted, and there is evidence of extra electronic absorption bands in the region $\lambda > 320$ nm. For the nitrosyl complexes, **2c** and **3c,** allowed low-energy bands of $a_{1u}(\pi), a_{2u}(\pi) \rightarrow NO(\pi^*)$ character are predicted and account for the observed extra bands. For other complexes, **2b, 3b, 3d,** and **3e,** the extra transitions are assigned as forbidden charge transfer transitions $(d,\pi^*)$; it is suggested that the phosphorescence of **3b** is due to a triplet excited state of this type. We are unable to account for the extra intense visible bands of the bispyridine complexes, **2a** and **3a,** by any one-electron transitions. The suggestion is made that these are due to doubly excited states of form $[e_g(d_\pi)]^3\,[a_{1u}(\pi),a_{2u}(\pi)]^3[e_g(\pi^*)]^2$, which mix with the ring singly excited states $[e_g(d_\pi)]^4\,[a_{1u}(\pi),-a_{2u}(\pi)]^3\,[e_g(\pi^*)]^1$.

**Acknowledgments.** The research was supported in part by Public Health Services Research Grants AM 16508, the Deutsche Forschungsgemeinschaft, and the Fonds der Chemischen Industrie (Federal Republic of Germany). We thank Professors Dr. H. H. Inhoffen (Braunschweig) and Dr. H. Pommer (BASF, Ludwigschafen) for a generous gift of octaethylporphyrin. The first emission studies on Os(OEP)-CO(py) were done by Dr. Daniel B. Howell.l. technical help with the computer was provided by James Van Zee, Charles Connell, and Dr. Frank Kampas.

## References and Notes

(1) Part 35: M. Gouterman, D. H. Holten, and E. Lieberman, *Chem. Phys.*, **25,** 139 (1977).
(2) (a) University of Washington, Seattle; (b) Technische Hochschule, Aachen.
(3) E. Antonini and M. Brunori, "Hemoglobin and Myoglobin in Their Reaction with Ligands", North-Holland Publishing Co., Amsterdam, 1971.
(4) F. Adar in "The Porphyrins", Vol. III, D. Dolphin, Ed., Academic Press, New York, N.Y., in press, Chapter 2.
(5) J. O. Alben, W. H. Fuchsman, C. A. Beaudreau, and W. S. Caughey, *Biochemistry,* **7,** 624 (1968).
(6) J. W. Buchler in "Porphyrins and Metalloporphyrins", K. M. Smith, Ed., Elsevier, Amsterdam, 1975; and in ref 4.
(7) M. Gouterman in ref 4, Chapter 1.
(8) J. W. Buchler and K. Rohbock, *J. Organomet. Chem.*, **65,** 223 (1974).
(9) J. W. Buchler and P. D. Smith, *Chem. Ber.*, **109,** 1465 (1976).
(10) J. W. Buchler and P. D. Smith, *Angew. Chem.*, **86,** 378 (1974); *Angew. Chem., Int. Ed. Engl.*, **13,** 341 (1974).
(11) J. W. Buchler and P. D. Smith, *Angew. Chem.*, **86,** 820 (1974); *Angew. Chem., Int. Ed. Engl.*, **13,** 745 (1974).
(12) B. C. Chow and I. A. Cohen, *Bioinorg. Chem.*, **1,** 57 (1971).
(13) M. Tsutsui, D. Ostfeld, and L. M. Hoffman, *J. Am. Chem. Soc.*, **93,** 1820 (1971).
(14) W. Sovocol, F. R. Hopf, and D. G. Whitten, *J. Am. Chem. Soc.*, **94,** 4350 (1972).
(15) Part 31: M. Gouterman, L. K. Hanson, G.-E. Khalil, J. W. Buchler, K. Rohbock, and D. Dolphin, *J. Am. Chem. Soc.*, **97,** 3142 (1975).
(16) Part 13: P. G. Seybold and M. Gouterman, *J. Mol. Spectrosc.*, **31,** 1 (1969).
(17) A. T. Gradyushko and M. P. Tsvirko, *Opt. Spektrosk.*, **31,** 548 (1971); *Opt. Spectrosc. (USSR)*, **31,** 291 (1971).
(18) C. R. Connell, Ph.D. Thesis, University of Washington, Seattle, 1977.
(19) Part 4: M. Zerner and M. Gouterman, *Theor. Chim. Acta,* **4,** 44 (1966).
(20) Part 21: A. M. Schaffer and M. Gouterman, *Theor. Chim. Acta,* **18,** 1 (1970).
(21) Part 34: P. Sayer, M. Gouterman, and C. R. Connell, *J. Am. Chem. Soc.,* **99,** 1082 (1977).
(22) L. C. Cusachs and J. H. Corrington in "Sigma Molecular Orbital Theory", O. Sinanoglu and K. B. Wiberg, Ed., Yale University Press, New Haven, Conn., 1970, pp 256–272.
(23) C. E. Moore, *Natl. Bur. Stand. (U.S.), Circ.,* **No. 467,** 1 (1949); **2** (1952), **3** (1958).
(24) S. P. McGlynn, L. G. Vanquickenborne, M. Kinoshita, and D. G. Carroll, "Introduction to Applied Quantum Chemistry", Holt, Rinehart and Winston, New York, N.Y. 1972, pp 106–113.
(25) L. J. Radonovich, A. Bloom, and J. L. Hoard, *J. Am. Chem. Soc.*, **94,** 2073 (1972).
(26) J. J. Bonnet, S. S. Eaton, G. R. Eaton, R. H. Holm, and J. A. Ibers, *J. Am. Chem. Soc.*, **95,** 2141 (1973).
(27) L. Pauling, "The Chemical Bond", Cornell University Press, Ithaca, N.Y., 1967, pp 135–153.
(28) F. R. Hopf, T. P. O'Brien, W. R. Scheidt, and D. G. Whitten, *J. Am. Chem. Soc.*, **97,** 277 (1975).
(29) J. W. Buchler, W. Kokisch, and P. D. Smith, *Struct. Bonding (Berlin)*, in press.
(30) The boundary between *normal* and *hypso* $\alpha$ bands has an overlap region of 565–570 nm for metallooctaethylporphyrins in solution.
(31) Part 27: M. Gouterman, F. P. Schwarz, P. D. Smith, and D. Dolphin, *J. Chem. Phys.*, **59,** 676 (1973); addendum, M. Gouterman and D. B. Howell, *ibid.*, **61,** 3491 (1974).
(32) L. K. Hanson, W. A. Eaton, S. G. Sligar, I. C. Gunsalus, M. Gouterman, and C. R. Connell, *J. Am. Chem. Soc.*, **98,** 2672 (1976).
(33) Part 1: M. Gouterman, *J. Mol. Spectrosc.*, **6,** 138 (1961).
(34) Part 3: C. Weiss, H. Kobayashi, and M. Gouterman, *J. Mol. Spectrosc.*, **16,** 415 (1965).
(35) Part 24: A. J. McHugh, M. Gouterman, and C. Weiss, Jr., *Theor. Chim. Acta,* **24,** 346 (1972).
(36) Part 18: D. Eastwood and M. Gouterman, *J. Mol. Spectrosc.*, **35,** 359 (1970).
(37) Part 29: L. K. Hanson, M. Gouterman, and J. C. Hanson, *J. Am. Chem. Soc.*, **95,** 4822 (1973).
(38) F. Adar, M. Gouterman, and S. Aronowitz, *J. Phys. Chem.*, **80,** 2184 (1976).
(39) W. A. Eaton and E. Charney, *J. Chem. Phys.*, **51,** 4502 (1969).
(40) Part 32: M. Gouterman, L. K. Hanson, G.-E. Khalil, and W. R. Leenstra, *J. Chem. Phys.*, **62,** 2343 (1975).
(41) P. D. Smith, Doctoral Dissertation, Technische Hochschule, Aachen, 1976.
(42) A. Antipas, Ph.D. Thesis, Department of Chemistry, University of Washington, Seattle, in preparation.
(43) L. J. Boucher, *Coord. Chem. Rev.*, **7,** 289 (1972).
(44) R. W. Harrigan, G. D. Hager, and G. A. Crosby, *J. Chem. Phys.*, **59,** 3468 (1973).
(45) R. W. Harrigan, G. D. Hager, and G. A. Crosby, *Chem. Phys. Lett.*, **21,** 487 (1973).
(46) M. Gouterman, *J. Chem. Phys.*, **33,** 1523 (1960).
(47) H. Kobayashi, T. Hara, and Y. Kaizu, *Bull. Chem. Soc. Jpn.*, **45,** 2148 (1972).
(48) H. Kobayashi, Y. Yanagawa, H. Osada, S. Minami, and M. Shimizu, *Bull. Chem. Soc. Jpn.*, **46,** 1471 (1973).
(49) H. Kobayashi, T. Higuchi, Y. Kaizu, H. Osada, and M. Aoki, *Bull. Chem. Soc. Jpn.*, **46,** 1471 (1973).
(50) H. Kobayashi, *Adv. Biophys.*, **8,** 191 (1975).
(51) H. Kobayashi, T. Higuchi, and K. Eguchi, *Bull. Chem. Soc. Jpn.*, **49,** 457 (1976).
(52) G. M. Brown, F. R. Hopf, J. A. Ferguson, T. J. Meyer, and D. G. Whitten, *J. Am. Chem. Soc.*, **95,** 5939 (1973).
(53) G. M. Brown, F. R. Hopf, T. J. Meyer, and D. G. Whitten, *J. Am. Chem. Soc.*, **97,** 5385 (1975).
(54) J. H. Fuhrhop, *Struct. Bonding (Berlin)*, **18,** 1 (1974).
(55) T. G. Spiro and J. M. Burke, *J. Am. Chem. Soc.*, **98,** 5482 (1976).
(56) NOTE ADDED IN PROOF. Lifetime measurements at 77 K in toluene snow show a nonexponential decay that can be fit as a sum of two exponential decays with lifetimes 103 and 21 $\mu$s.